Bioorganic Chemistry 92 (2019) 103215

Contents lists available at ScienceDirect

Bioorganic Chemistry

journal homepage: www.elsevier.com/locate/bioorg

A dual-emission fluorescent probe for discriminating cysteine from homocysteine and glutathione in living cells and zebrafish models

Zhengliang Lu, Yanan Lu, Xin Sun, Chunhua Fan*, Zongyi Long, Liying Gao

School of Chemistry and Chemical Engineering, University of Jinan, Jinan 250022, China

ARTICLE INFO

Keywords:
Dual-emission fluorescent probe
Discrimination of biothiols
NBD, Living cell
Zebrafish models

ABSTRACT

Cellular biothiols function crucially and differently in physiological and pathological processes. However, it is still challenging to detect and discriminate thiols within a single one molecule, especially for cysteine (Cys) and homocysteine (Hcy). In this study, a simple two-emission turn-on fluorescent biothiol probe (**ICN-NBD**) was rationally designed and synthesized through a facile ether bond linking 7-nitro-1,2,3-benzoxadiazole (NBD) and phenanthroimidazole containing a cyano tail. The probe in the presence of Cys elicited two fluorescence responses at 470 nm and 550 nm under excitation at 365 nm and 480 nm, respectively, because of the concomitant generation of both the fluorophore and **NBD-*N*-Cys.** In contrast, addition of Hcy and glutathione (GSH) could result in only a blue fluorescence enhancement at 470 nm. which was reasonably attributed to rearrangement from **NBD-*S*-Hcy/GSH** to **NBD-*N*-Hcy/GSH** as a result of geometrical constraints or solvent effects. Therefore, the fluorescent probe with the NBD scaffold could detect biothiols and simultaneously discriminate Cys from Hcy/GSH in both blue and green channels. The probe has been successfully applied for visualizing biothiols in living cells and zebrafish.

1. Introduction

The study of reactive sulfur species (RSS) in biological systems, especially cysteine (Cys), homocysteine (Hcy) and glutathione (GSH) has been attracting much attention due to their crucial roles in physiological and pathological processes [1–3]. Among them, Cys participates in cell growth and in the synthesis and increased rigidity of proteins as well as chelation of metal ions in enzymes [4–6]. In the presence of cystathionine β-synthase (CBS), cystathionine γ-lyase (CSE), and 3-mercaptopyruvate sulfur transferase (3-MST), Cys could be catalytically transformed into the endogenous gaseous transmitter H_2S which has been implicated in the induction of hippocampal long-term potentiation, brain development, and blood pressure regulation [7]. With assistance of γ-glutamylcysteine synthetase (GSH I) and glutamine synthetase (GSH II), Cys is involved in the formation of the antioxidant GSH maintains cellular redox homeostasis and protects thiol-containing proteins and enzymes from reactive oxygen species, such as free radicals and peroxides, as well as heavy metals through reversible oxidization of glutathione disulfide (GSSG) [8]. Hcy can be catalytically converted into Cys by CBS and CSE with the aid of Vitamin B_6 [9]. Imbalance of biothiols is involved in edema, retarded growth rate, liver damage, leucocyte loss, psoriasis, Alzheimer's disease and down's syndrome [10–14]. Therefore, it is meaningful and important to be able to conveniently and sensitively detect and simultaneously discriminate biothiols in clinic diagnostics and pathophysiology exploration.

Compared with conventional detection methods including high-performance liquid chromatography, electrochemical assay, and mass spectrometry [15–17], fluorescence spectroscopy offers many advantages including simplification, high sensitivity and low cost, non-invasiveness, high spatial resolution and notably, visualization of the target of interest in a biological environment [18–25]. In this regard, various mechanisms including Michael addition, cleavage of sulfonamide and sulfonate ester, cyclization with aldehyde, and others, have been used to construct numerous fluorescent probes for biothiols [26–38]. Due to their similar structure and reaction sites, most fluorescent probes could respond to only one or two of the biothiols. Therefore, discrimination of biothiols is still a big challenge although several probes have been developed for biothiols using multiple reaction sites in one molecule [39–43]. It is worth noting that most probes are single-emission or intensity-based fluorescent probes which could usually suffer at least one of the drawbacks, such as low selectivity and sensitivity, a high limit of detection, large volumes of organic solvent, and/or short excitation/emission wavelengths. However, dual-emission fluorescent probes would be more accurate because of the good built-in self-calibration to effectively eliminate the interference from environmental conditions and biological systems [44–48]. Unfortunately, few

* Corresponding author.
E-mail address: chm_fanch@ujn.edu.cn (C. Fan).

https://doi.org/10.1016/j.bioorg.2019.103215
Received 25 March 2019; Received in revised form 9 July 2019; Accepted 21 August 2019
Available online 23 August 2019
0045-2068/

dual-emission fluorescent probes have been reported for discriminating biothiols [49–53]. For instance, Lin and co-workers developed a dual-emission fluorescent probe for discrimination of biothiols and H_2S in phosphate-buffered saline (PBS) containing 20% acetonitrile [49]. Wu and co-workers reported a hemicyanine fluorescent probe for distinguishing Cys/Hcy from GSH in 5% DMSO/PBS [50]. Very recently, Song and co-workers designed a multi-emission fluorescent probe for discriminatory detection of Cys/Hcy, GSH/H_2S, and thiophenol [51]. However, these fluorescent probes failed to distinguish between Cys and Hcy. It is clear that the selectivity of a probe toward the target of interest can be significantly affected by minor changes of a moiety within the probe [54–57]. Thus, we envisioned that introduction of a suitable electron-withdrawing group within a dual-emission fluorescent probe could induce a remarkable shift of emission wavelength after reaction with biothiols. Based on this hypothesis and our former research [58], we synthesized a simple dual-emission fluorescent probe for biothiols by anchoring 7-nitro-1,2,3-benzoxadiazole (NBD) to a cyano-phenanthroimidazole fluorophore. The initial nucleophilic attack of biothiols toward the ether bond of the probe would release the phenanthroimidazole fluorophore with emission at 470 nm upon excitation at 365 nm. Due to the solvent impact and/or geometrical difference between Cys and Hcy/GSH, an intramolecular cyclization-rearrangement cascade reaction took place in the presence of only Cys, eliciting a remarkable green fluorescence at 550 nm (Ex 480 nm) (see Scheme 1). Therefore, the probe **ICN-NBD** could detect biothiols and further discriminate Cys from Hcy/GSH in both blue and green channels. Moreover, the probe was successfully applied for visualizing biothiols in living HeLa cells and zebrafish models.

2. Experimental

2.1. Materials and instruments

All reagents and chemicals were commercially obtained from suppliers. NMR spectra were carried out on a Bruker spectrometer. ESI-HRMS were recorded on a Bruker Daltonics APEX II 47e FT-ICR spectrometer. UV-vis and Fluorescence spectra were measured on a TU-1901 spectrometer and F-380 luminescence spectrometer, respectively. The cells were imaged by a confocal laser scanning microscope. Phenanthroimidazole fluorophore was obtained according to the literature [59].

2.2. Synthesis of *ICN-NBD*

Compound **ICN-OH** (0.41 g, 1 mmol) and **NBD-Cl** (0.40 g, 2 mmol) was dissolved in dry dichloromethane (10 mL) under a nitrogen atmosphere. Triethylamine (0.33 mL) was added and the mixture was stirred ambiently overnight. The residue was purified by flash chromatography using EtOAc/pet. ether (v/v 1:4) to afford the pure compound **ICN-NBD** as a blue solid (0.28 g, yield 49%). ^{1}H NMR (400 MHz, $CDCl_3$) δ 8.94 – 8.84 (m, 2H), 8.59 (d, J = 7.8 Hz, 1H), 8.46 (d, J = 2.4 Hz, 1H), 8.40 (d, J = 8.3 Hz, 1H), 8.26 (d, J = 7.7 Hz, 1H), 8.07 (dd, J = 8.7, 2.5 Hz, 1H), 8.01 (d, J = 5.0 Hz, 3H), 7.79 (t, J = 7.4 Hz, 1H), 7.73–7.70 (m, 1H), 7.66 (dt, J = 5.7, 3.6 Hz, 1H), 7.56 (t, J = 7.7 Hz, 1H), 7.47 (d, J = 8.7 Hz, 1H), 7.22 (t, J = 7.6 Hz, 1H), 7.10 (d, J = 8.3 Hz, 1H), 6.66 (d, J = 8.4 Hz, 1H). ^{13}C NMR (101 MHz, $CDCl_3$) δ 151.66, 150.57, 148.40, 146.25, 144.54, 143.78, 143.36, 142.54, 139.09, 138.67, 137.37, 133.13, 132.99, 132.76, 132.59, 131.55, 130.90, 130.41, 130.08, 129.82, 128.83, 128.68, 127.82, 126.95, 126.75, 126.24, 124.68, 124.46, 123.29, 122.60, 121.89, 121.41, 120.42, 118.37, 109.56. MS (ESI, m/z) Calcd for $[C_{34}H_{18}N_6O_4\text{-}H]^+$, 573.1311; found, 573.1350.

2.3. HeLa cells and zebrafish imaging

HeLa cells were seeded on glass-bottomed dishes in culture media for 24 h. The cultured cells were washed twice by PBS before subsequent experiments and divided into four groups. In a control group,

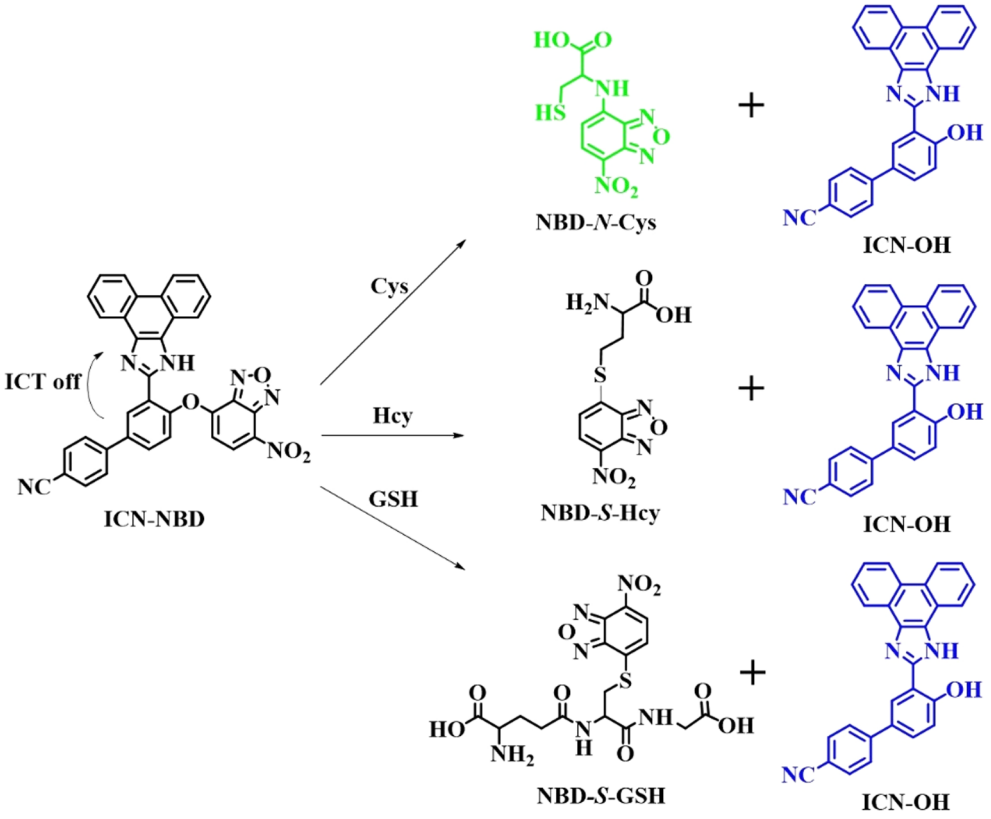

Scheme 1. Proposed recognition mechanism of **ICN-NBD** towards biothiols.

HeLa cells were incubated with 100 μM *N*-ethylmaleimide (NEM) for 30 min and then **ICN-NBD** (20 μM) at 37 ℃ for another 30 min. In the second group, the HeLa cells were treated with the probe (20 μM) for 30 min after incubation with NEM (100 μM) for 30 min and then Cys (20 μM) for another 30 min. In the third group, HeLa cells pretreated with 100 μM NEM for 30 min and then with Hcy (50 μM) for another 30 min were incubated with the probe (20 μM) for 30 min. In the fourth group, HeLa cells were cultured with NEM (100 μM) for 30 min, and subsequently incubated with GSH (50 μM) for 30 min, and finally with the probe (20 μM) for 30 min. After washing, HeLa cell images were taken using a confocal laser scanning microscope. Zebrafish were imaged after incubation with NEM (500 μM), the probe (20 μM), or biothiols (50 μM) for 30 min, respectively.

3. Results and discussion

3.1. Rational design and synthesis of *ICN-NBD*

Although several probes relying on multiple reaction sites have been developed for discriminating biothiols, it is still challenging to simultaneously discriminate between them [60]. In contrast, dual-emission fluorescent probes due to the build-in self-calibration pave a more promising way for detecting biothiols and even distinguishing Cys and Hcy [50–51]. These previous studies containing the NBD moiety demonstrated a similar cyclization rearrangement cascade reaction with Cys and Hcy. We imagined that the cyano group of the probe could affect the emission wavelength of the fluorophore. Considering that NBD acts as both a good indicator and biothiol-sensing group, the probe **ICN-NBD** with a cyano group tail was synthesized through a one-step reaction between NBD-Cl and **ICN-OH** in the presence of Et_3N. **ICN-NBD** was fully characterized by ^1H NMR, ^{13}C NMR and HRMS (Fig. S1–S3).

3.2. Sensing properties of *ICN-NBD* toward biothiols

With compound **ICN-NBD** in hand, the fluorescence responses of the probe were initially investigated in the presence and absence of biothiols in DMF-H_2O (v/v, 4:6, 20 mM PBS buffer; pH 7.4). Free **ICN-NBD** (10 μM) displayed no fluorescence upon excitation at both 365 nm and 480 nm. However, addition of biothiols to media containing **ICN-NBD** induced strong fluorescence changes. As shown in Fig. 1a, in the presence of Cys, the probe demonstrated two independent fluorescence enhancements at 470 and 550 nm when excited at 365 and 480 nm, respectively. The fluorescence in blue and green channels increased and reached a maximum plateau at 470 and 550 nm, respectively, in the presence of 10 equiv. of Cys. In contrast, only blue fluorescence at 470 nm was observed upon excitation at 365 nm in the presence of Hcy and GSH (Fig. 1b and c). The strong blue fluorescence confirmed that the nucleophilic substitution reaction was successfully initiated, which emitted fluorescence at 470 nm due to released **ICN-OH**. The probe showed very weak fluorescence at 550 nm with Hcy and GSH upon excitation at 480 nm. The maximum emission intensities at 470 nm were obtained with addition of 10 equiv. of Hcy and 18 equiv. of GSH. Compared with Cys, the weak green fluorescence of **ICN-NBD** with Hcy and GSH was probably attributed to the unfavorable transformation from **NBD-*S*-Hcy** and **NBD-*S*-GSH** to **NBD-*N*-Hcy** and **NBD-*N*-GSH**, respectively. This is likely due to the influence of steric or solvent interactions as has been observed in previous work for similar probes [61]. Moreover, good linear relationships were obtained between the fluorescence intensities at 470 nm of the probe and the concentration of Cys, Hcy, and GSH in the range of 0–100 μM, 0–100 μM, and 0–180 μM, respectively (Fig. S4). The corresponding limits of detection were estimated to be 22.6 nM for Cys, 31.2 nM for Hcy, and 17.7 nM for GSH, respectively. These results indicate that the probe could quantitatively detect biothiols and further discriminate Cys from Hcy and GSH.

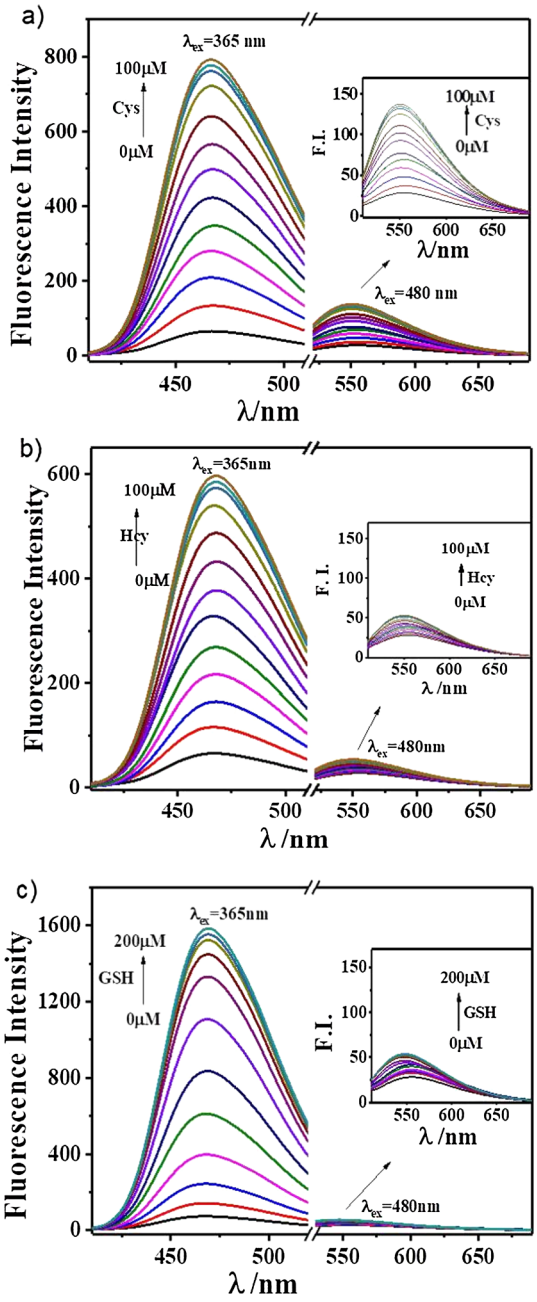

Fig. 1. Fluorescence spectra of **ICN-NBD** (10 μM) with gradual addition of Cys (a), Hcy (b) and GSH (c), respectively, in DMF-PBS (v/v, 4:6, 20 mM PBS, pH 7.4).

3.3. Selectivity of *ICN-NBD* toward biothiols

In order to prove excellent selectivity toward biothiols, the fluorescence responses of **ICN-NBD** (10 μM) were investigated with biologically relevant species in DMF-buffer solution (4:6, v/v, PBS 20 mM, pH 7.4). As shown in Fig. 2a, the probe showed strong fluorescence at 470 nm in the presence of biothiols (Cys, Hcy, and GSH). Related interfering species, such as thiophenol (PhSH), Na_2S, other amino acids (200 μM) (Asp, l-Try, Gly, Val, Ile, Glu, Arp, Leu, Ala, His, Lys, Met, Phe, Tyr, Ser, Pro, Try and Thr) and common species (H_2O_2, F^-, I^-, Cl^-, SO_4^{2-}, SO_3^{2-}, AcO^-, K^+, Na^+, Al^{3+}, Mg^{2+}, Zn^{2+}, Cr^{3+}, Hg^{2+}, Ba^{2+}, Cu^{2+}, Fe^{2+}, Mn^{2+}, Cd^{2+}, Fe^{3+} and Ca^{2+}), did not induce significant fluorescence emission. It is to be noted that only Cys led to a strong emission intensity at 550 nm although Hcy and GSH resulted in weak green

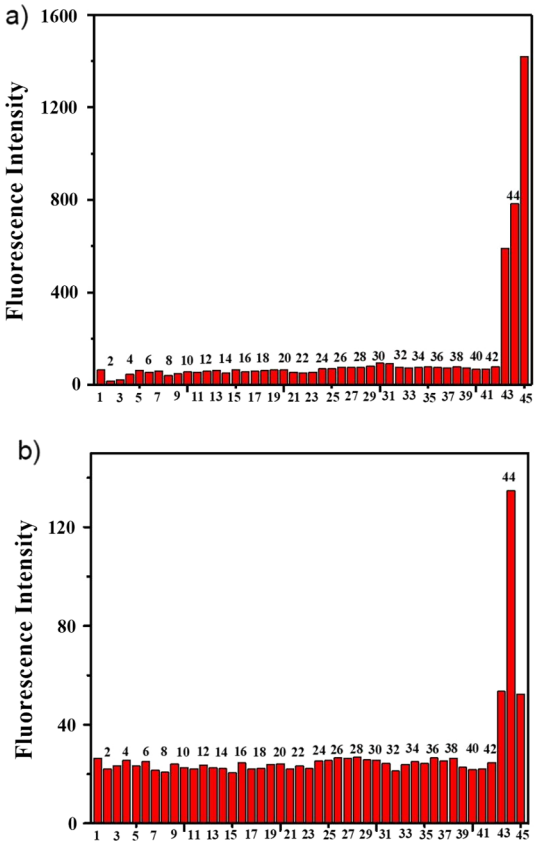

Fig. 2. Fluorescence intensity at 470 nm (a) and 550 nm (b) of **ICN-NBD** (10 μM) upon addition of biothiols and other interfering species upon excitation at 365 nm and 480 nm, respectively. From left to right, 1. Blank, 2·H_2O_2, 3. F^-, 4. I^-, 5. Cl^-, 6. SO_4^{2-}, 7. SO_3^{2-}, 8. AcO^-, 9. K^+, 10. Na^+, 11. Al^{3+}, 12. Mg^{2+}, 13. Zn^{2+}, 14. Cr^{3+}, 15. Hg^{2+}, 16. Ba^{2+}, 17. Cu^{2+}, 18. Fe^{2+}, 19. Mn^{2+}, 20. Cd^{2+}, 21. Fe^{3+}, 22. Ca^{2+}, 23. Asp, 24. l-Try, 25. Gly, 26. Val, 27. Ile, 28. Glu, 29. Arp, 30. Leu, 31. Ala, 32. His, 33. Lys, 34. Met, 35. Phe, 36. Tyr, 37. Ser, 38. Pro, 39. Try, 40. Thr, 41. PhSH, 42. Na_2S, 43. Hcy, 44. Cys, 45. GSH.

fluorescence (Fig. 2b). These results indicate that the probe could not only detect biothiols over the other related interfering species but also discriminate Cys from Hcy/GSH.

The effect of pH on the fluorescence response at 470 nm of the probe in the absence or presence of 20 equiv. of biothiols was explored in 40% DMF aqueous solution in order to extend potential applications in biological systems (Fig. S5). It was found that free probe **ICN-NBD** did not elicit any significant fluorescence at 470 nm in the pH range from 2.0 to 12.0, which demonstrated the stability of the probe. As expected, addition of 20 equiv. of biothiols resulted in strong blue fluorescence at 470 nm of the probe in the pH range from 5.0 to 10.0. However, the fluorescence of the probe at 470 nm was silent with biothiols in more acidic (pH < 5.0) or basic environment (pH greater than 10.0) which probably inhibited the aromatic substitution reaction between the probe and biothiols. This wide working pH range of 5.0–10.0 indicates that the probe can work well under physiological conditions.

As a crucial parameter of reaction-based probes, response time was checked by investigating the fluorescence of the probe at 470 nm in the presence of biothiols at different concentration over time. As shown in Fig. S6, addition of biothiols at different concentration such as Cys (50 and 100 μM), Hcy (50 and 100 μM) and GSH (100 and 200 μM) induced a gradual fluorescence enhancement of the probe and finally reached a plateau in approximately 30 min. These time-course fluorescence measurements of the probe evidenced that response time is almost independent of the biothiol concentration.

3.4. The proposed sensing mechanism of *ICN-NBD* towards biothiols

At present, numerous single-emission fluorescent probes for biothiols have been developed whose further potential application was limited due to a lack of built-in self-calibration, although a few probes have been designed for discriminating biothiols based on multi reaction sites [62–64]. Fortunately, several groups have shown that dual-emission fluorescent probes are a promising tool due to high accuracy from their built-in self-calibration, when they followed a popular strategy of combining a good indicator and recognition group NBD with other fluorophores [50,52]. An aromatic nucleophilic substitution reaction can readily break the ether bond of the probes and release the fluorophore **ICN-OH** and NBD-containing intermediates thereby emitting blue fluorescence at 470 nm (ex 365 nm) by switching on intramolecular charge transfer (ICT). It should be noted that these fluorescent probes could discriminate Cys/Hcy from GSH because both NBD-containing intermediates (**NBD-S-Cys** and **NBD-*S*-Hcy**) can undergo a cyclization and substitution cascade reaction that is not observed for **NBD-*S*-GSH.** The probe **ICN-NBD** was synthesized by anchoring NBD to the cyano-fluorophore (**ICN-OH**). To gain insight into the sensing mechanism, the HRMS spectra of **ICN-NBD** in the presence of Cys, Hcy, and GSH, were performed. As shown in Fig. S7, the spectra of **ICN-NBD** with GSH presented a peak at m/z = 410.13026 assigned to the fluorophore ([**ICN-OH**-H^+]: Calcd 410.12934) and a peak at m/z = 469.07870 corresponding to the species **NBD-*S*-GSH** ([**NBD-*S*-GSH**-H^+]: Cald 469.07777), an expected compound regardless of steric factor. Besides the peak at 410.12967 from the fluorophore ([**ICN-OH**-H^+]: Calcd 410.12989), HRMS spectra of **ICN-NBD** in the presence of Cys also demonstrated a new peak at 283.01419 reasonably attributed to **NBD-*N*-Cys** ([**NBD-*N*-Cys**-H^+]: Calcd 283.03172) which is good agreement with literatures (Fig. S8) [51,65]. Surprisingly, addition of Hcy to the probe can produce the fluorophore and the nonfluorescent species **NBD-*S*-Hcy** which was scarcely transformed into florescent **NBD-*N*-Hcy** as observed in Fig. 1b. This phenomenon was reasonably attributed to the influence from geometrical constraints and/or solvent interaction [61]. As shown in Fig. S9, addition of all three biothiols to the probe led to an absorption peak at 365 nm, which was assigned to **ICN-OH.** Notably, reaction between **ICN-NBD** and GSH resulted in a broad absorption shoulder at about 420 nm corresponding to the nonfluorescent **NBD-*S*-GSH.** Addition of Hcy to the probe produced a new broad absorption band at 446 nm from nonfluorescent **NBD-*S*-Hcy.** This designation was further confirmed by a Cys-induced absorption peak at 470 nm corresponding to fluorescent **NBD-*N*-Cys.** Thus, these results strongly support the proposed recognition mechanism of the probe toward biothiols.

3.5. Imaging biothiols in living cells and zebrafish

The excellent selectivity and sensitivity of the probe toward biothiols in vitro under simulated physiological conditions encouraged us to further explore its potential application in biological systems. The cytotoxicity effect of probe **ICN-NBD** was initially checked by a standard MTT assay in living HeLa cells. After incubation with **ICN-NBD** at different concentration ranging from 0 to 20 μM for 24 h, HeLa cells did not show any major loss of viability (Fig. S10). Indeed, the cell viability is still more than 90% after incubation with up to 20 μM of probe. These results show the low cytotoxicity and good permeability of **ICN-NBD** in living HeLa cells.

Next, we carried out a series of cell experiments to check whether the probe could visualize biothiols in HeLa cells by utilizing a confocal laser scanning microscope (Leica Microsystems). In a control group, HeLa cells were incubated with NEM, a well-known thiol-specific scavenger, for 30 min, and subsequently with the probe (20 μM) for another 30 min. As shown in Fig. 3a–d, there was not any obvious fluorescence in both blue and green channels observed. This indicated that NEM successfully deplete the endogenous biothiols. Subsequently, HeLa

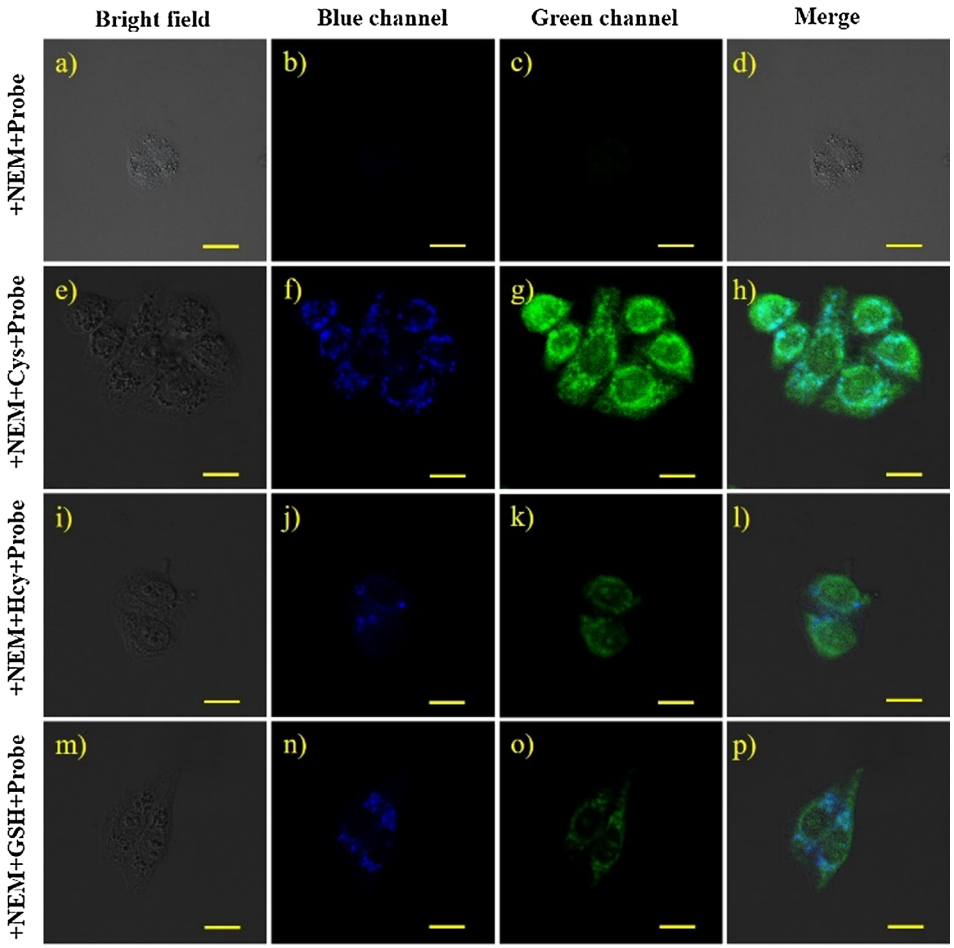

Fig. 3. Confocal Fluorescence images of living HeLa cells in blue and green channels. (a–c) HeLa cells incubated with NEM (100 μM) and then **ICN-NBD** (20 μM). (d) Overlay of a–c. (e–g) HeLa cells incubated with NEM (100 μM), then Cys (50 μM), and then **ICN-NBD** (20 μM). (h) Overlay of e–g. (i–k) HeLa cells incubated with NEM (500 μM), then Hcy (50 μM), and then **ICN-NBD** (20 μM). (l) Overlay of i–k. (m–o) HeLa cells incubated with NEM (100 μM), then GSH (50 μM), and then **ICN-NBD** (20 μM). (p) Overlay of m-o. Blue and green channels correspond to the emission windows of 420–470 and 500–550 nm, respectively. Excitation at 405 and 488 nm, respectively. Scale bar = 20 μm.

cells were incubated with the probe for 30 min after treatment with NEM (100 μM) and then Cys (50 μM). The cells showed strong fluorescence in both blue and green channels (Fig. 3e–h). In subsequent groups (Fig. 3i–p), the cells demonstrated strong fluorescence at 470 nm when HeLa cells were treated with the probe (20 μM) after incubation with NEM and then Hcy (50 μM) or GSH (50 μM). this group of cells presented very weak green fluorescence. These results indicate that **ICN-NBD** can selectively bioimage biothiols based on the blue fluorescence in living cells and could also differentiate Cys from Hcy/GSH depending on the green fluorescence.

Inspired by the prominent above-mentioned fluorescence imaging in living HeLa cells, the feasibility of ICN-NBD for bioimaging biothiols was further checked in living zebrafish models. In a control group, 2-day-old zebrafish were incubated with NEM (500 μM) for 30 min and then with the probe (20 μM) for another 30 min. As show in Fig. 4a1–a4, zebrafish did not emit any significant fluorescence in both blue and green channels. In the experimental group, zebrafish were first incubated with NEM (500 μM) for 30 min and then treated with Cys (50 μM) for another 30 min followed by the probe (20 μM) for 30 min. As shown in Fig. 4b1–b4, both strong blue and green fluorescence was detected in zebrafish incubated with Cys. Zebrafish incubated with the probe after pretreatment with NEM and Hcy or GSH demonstrated strong blue fluorescence (Fig. 4c1–c4 and d1–d4). Only weak green fluorescence was detected. These results suggested that **ICN-NBD** could be successfully applied for visualizing biothiols in zebrafish.

4. Conclusion

In summary, this study has developed a simple dual-emission fluorescent probe for biothiols, based on combining two fluorophores nitrobenzofurazan (NBD) and phenanthroimidazole with a facile ether bond. In the presence of Cys, the probe emitted remarkable fluorescence in both blue (470 nm) and green (550 nm) channels. However, the addition of Hcy and GSH could only induce strong blue fluorescence, which was reasonably assigned to the influence from geometrical constraints and/or weak solvent interaction. These interesting findings demonstrate the probe could be a promising and effective tool to detect biothiols and further discriminate Cys from Hcy/GSH through a dual-emission mode. Moreover, the probe has been successfully applied for visualizing endogenous and exogenous biothiols in living HeLa cells and zebrafish models with low cytotoxicity and good membrane permeability.

Acknowledgements

We thank for the supporting from Shandong Provincial Natural Science Foundation of China (grant No. ZR2019MB040), the Science and Technology Project of University of Jinan (Grant No. XKY1823 and XBS1320). We also thank Dr. Cory A. Black at BDG Synthesis (PO Box 38627, Wellington Mail Centre, Wellington 5045, New Zealand) for his suggestions and comments which allowed us to largely improve the manuscript.

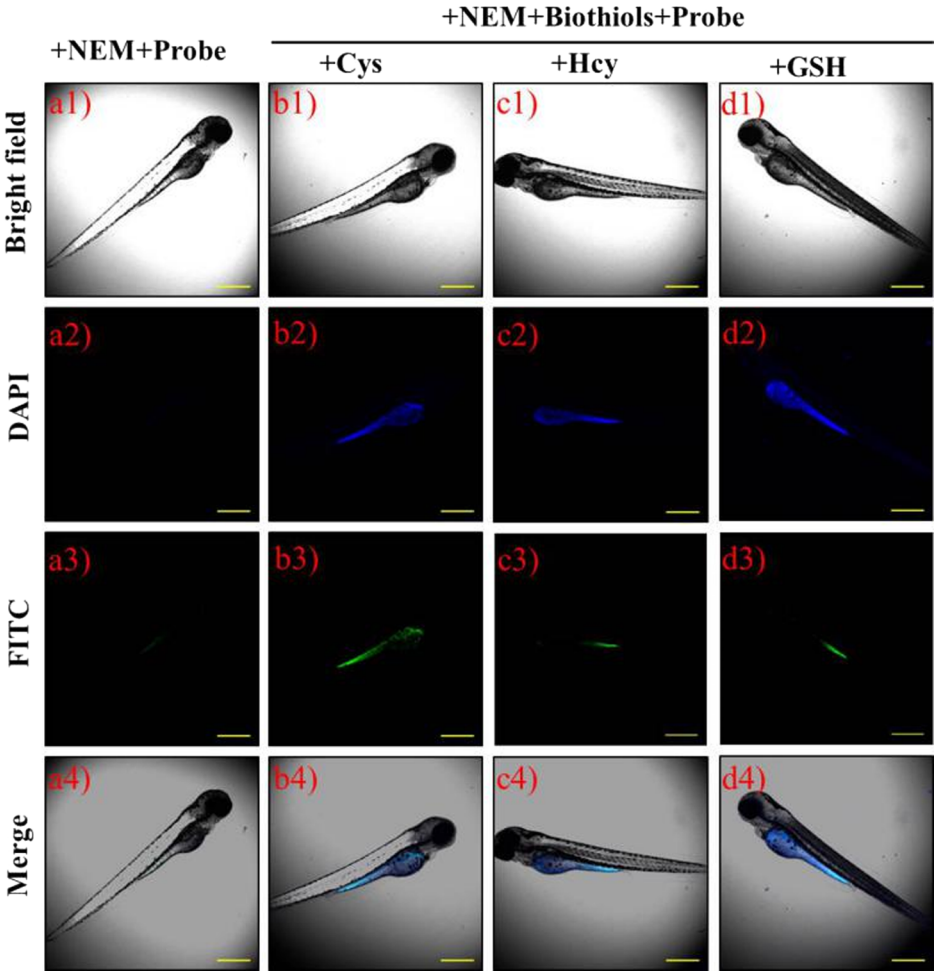

Fig. 4. Fluorescence images of zebrafish. a1–a4) Zebrafish only for comparison. (B1–b4) Zebrafish incubated with NEM (500 μM) and then **ICN-NBD** (20 μM). (c1–c4) Zebrafish with Cys (50 μM). d1–d4) Zebrafish with Hcy (50 μM). (e1–e4) Zebrafish incubated with GSH (50 μM). Scale bar = 500 μm.

Appendix A. Supplementary material

Supplementary data to this article can be found online at https://doi.org/10.1016/j.bioorg.2019.103215.

References

[1] T.V. Mishanina, M. Libiad, R. Banerjee, Biogenesis of reactive sulfur species for signaling by hydrogen sulfide oxidation pathways, Nat. Chem. Biol. 11 (2015) 457–464.

[2] X. Chen, Y. Zhou, X. Peng, J. Yoon, Fluorescent and colorimetric probes for detection of thiols, Chem. Soc. Rev. 39 (2010) 2120–2135.

[3] K. Ckless, Redox proteomics: from bench to bedside, Adv. Exp. Med. Biol. 806 (2014) 301–317.

[4] H.M. Fischer, T. Bruderer, H. Hennecke, Essential and non-essential domains in the Bradyrhizobium japonicum NifA protein: identification of indispensable cysteine residues potentially involved in redox reactivity and/or metal binding, Nucleic Acids Res. 16 (1988) 2207–2224.

[5] N. Wang, C.Y. Majmudar, W.C. Pomerantz, J.K. Gagnon, J.D. Sadowsky, J.L. Meagher, T.K. Johnson, J.A. Stuckey, C.L. Brooks, J.A. Wells, A.K. Mapp, Ordering a dynamic protein via a small-molecule stabilizer, J. Am. Chem. Soc. 135 (2013) 3363–3366.

[6] W. Droege, Oxidative stress and ageing: is ageing a cysteine deficiency syndrome? Philos. Trans. R. Soc. London, Ser. B 360 (2005) 2355–2372.

[7] R. Wang, Two's company, three's a crowd: can H2S be the third endogenous gaseous transmitter? FASEB J. 16 (2002) 1792–1798.

[8] M.H. Lee, Z. Yang, C.W. Lim, Y.H. Lee, D. Sun, C. Kang, J.S. Kim, Disulfide-cleavage-triggered chemosensors and their biological applications, Chem. Rev. 113 (2013) 5071–5109.

[9] M. Sibrian-Vazquez, J.O. Escobedo, S. Lim, G.K. Samoei, R.M. Strongin, Homocystamides promote free-radical and oxidative damage to proteins, Proc. Natl. Acad. Sci. 107 (2010) 551–554.

[10] E. Weerapana, C. Wang, G.M. Simon, F. Richter, S. Khare, M.B.D. Dillon, D.A. Bachovchin, K. Mowen, D. Baker, B.F. Cravatt, Quantitative reactivity profiling predicts functional cysteines in proteomes, Nature 468 (2010) 790–795.

[11] H. Tapiero, D.M. Townsend, K.D. Tew, The antioxidant role of selenium and seleno-compounds, Biomed. Pharmacother. 57 (2003) 134–144.

[12] D. Gong, S.-C. Han, A. Iqbal, J. Qian, T. Cao, W. Liu, W. Liu, W. Qin, H. Guo, Fast and selective two-stage ratiometric fluorescent probes for imaging of glutathione in living cells, Anal. Chem. 89 (2017) 13112–13119.

[13] Y.-W. Wang, S.-B. Liu, W.-J. Ling, Y. Peng, A fluorescent probe for relay recognition of homocysteine and group IIIA ions including Ga(III), Chem. Commun. 52 (2016) 827–830.

[14] D. Zhang, Z. Yang, H. Li, Z. Pei, S. Sun, Y. Xu, A simple excited-state intramolecular proton transfer probe based on a new strategy of thiol-azide reaction for the selective sensing of cysteine and glutathione, Chem. Commun. 52 (2016) 749–752.

[15] A.R. Ivanov, I.V. Nazimov, L.A. Baratova, Qualitative and quantitative determination of biologically active low-molecular-mass thiols in human blood by reversed-phase high-performance liquid chromatography with photometry and fluorescence detection, J. Chromatogr. A 870 (2000) 433–442.

[16] M.J. MacCoss, N.K. Fukagawa, D.E. Matthews, Measurement of homocysteine concentrations and stable isotope tracer enrichments in human plasma, Anal. Chem. 71 (1999) 4527–4533.

[17] W. Wang, J.O. Escobedo, C.M. Lawrence, R.M. Strongin, Direct detection of homocysteine, J. Am. Chem. Soc. 126 (2004) 3400–3401.

[18] C. Zhan, G. Zhang, D. Zhang, Zincke's salt-substituted tetraphenylethylenes for fluorometric turn-on detection of glutathione and fluorescence imaging of cancer cells, ACS Appl. Mater. Interfaces 10 (2018) 12141–12149.

[19] T.-B. Ren, W. Xu, W. Zhang, X.-X. Zhang, Z.-Y. Wang, Z. Xiang, L. Yuan, X.-B. Zhang, A general method to increase stokes shift by introducing alternating vibronic structures, J. Am. Chem. Soc. 140 (2018) 7716–7722.

[20] S. Ding, G. Feng, Smart probe for rapid and simultaneous detection and discrimination of hydrogen sulfide, cysteine/homocysteine, and glutathione, Sens. Actuat. B 235 (2016) 691–697.

[21] X. Yang, Y. Guo, R.M. Strongin, Conjugate addition/cyclization sequence enables selective and simultaneous fluorescence detection of cysteine and homocysteine, Angew. Chem., Int. Ed. 50 (2011) 10690–10693.

[22] K. Dou, G. Chen, F. Yu, Y. Liu, L. Chen, Z. Cao, T. Chen, Y. Li, J. You, Bright and sensitive ratiometric fluorescent probe enabling endogenous FA imaging and

mechanistic exploration of indirect oxidative damage due to FA in various living systems, Chem. Sci. 8 (2017) 7851–7861.
[23] K. Dou, Q. Fu, G. Chen, F. Yu, Y. Liu, Z. Cao, G. Li, X. Zhao, L. Xia, L. Chen, H. Wang, J. You, A novel dual-ratiometric-response fluorescent probe for SO_2/ClO- detection in cells and in vivo and its application in exploring the dichotomous role of SO_2 under the ClO- induced oxidative stress, Biomaterials 133 (2017) 82–93.
[24] L.L. Wang, Y. Qu, Y.X. Yang, J. Cao, L. Wang, A tetrasulphite-containing fluorescent chemodosimeter for Hg2+ with optimized selectivity towards Ag+, Sens. Actuator B-Chem. 269 (2018) 78–86.
[25] Y. Qu, X. Zhang, L.L. Wang, H.R. Yang, L. Yang, J. Cao, J.L. Hua, A phenazine-based near-infrared (NIR) chemodosimeter for cysteine obtained via a carbonyl-assisted cycloaddition process, Rsc Adv 6 (2016) 22389–22394.
[26] J. Zhang, X. Ji, H. Ren, J. Zhou, Z. Chen, X. Dong, W. Zhao, Meso-heteroaryl BODIPY dyes as dual-responsive fluorescent probes for discrimination of Cys from Hcy and GSH, Sens. Actuators, B 260 (2018) 861–869.
[27] X. Xie, M. Li, F. Tang, Y. Li, L. Zhang, X. Jiao, X. Wang, B. Tang, Combinatorial strategy to identify fluorescent probes for biothiol and thiophenol based on diversified pyrimidine moieties and their biological applications, Anal. Chem. 89 (2017) 3015–3020.
[28] S. Feng, Y. Fang, W. Feng, Q. Xia, G. Feng, A colorimetric and ratiometric fluorescent probe with enhanced near-infrared fluorescence for selective detection of cysteine and its application in living cells, Dyes Pigm. 146 (2017) 103–111.
[29] Z.-H. Fu, X. Han, Y. Shao, J. Fang, Z.-H. Zhang, Y.-W. Wang, Y. Peng, Fluorescein-based chromogenic and ratiometric fluorescence probe for highly selective detection of cysteine and its application in bioimaging, Anal. Chem. 89 (2017) 1937–1944.
[30] X. Ren, H. Tian, L. Yang, L. He, Y. Geng, X. Liu, X. Song, Fluorescent probe for simultaneous discrimination of Cys/Hcy and GSH in pure aqueous media with a fast response under a single-wavelength excitation, Sens. Actuat. B 273 (2018) 1170–1178.
[31] L. Rong, C. Zhang, Q. Lei, H.-L. Sun, S.-Y. Qin, J. Feng, X.-Z. Zhang, Long-term thiol monitoring in living cells using bioorthogonal chemistry, Chem. Commun. 51 (2015) 388–390.
[32] Z. Yang, Y. He, J.-H. Lee, N. Park, M. Suh, W.-S. Chae, J. Cao, X. Peng, H. Jung, C. Kang, J.S. Kim, A self-calibrating bipartite viscosity sensor for mitochondria, J. Am. Chem. Soc. 135 (2013) 9181–9185.
[33] Y. Tian, B. Zhu, W. Yang, J. Jing, X. Zhang, A fluorescent probe for differentiating Cys, Hcy and GSH via a stepwise interaction, Sens. Actuat. B 262 (2018) 345–349.
[34] Q. Chen, C. Jia, Y. Zhang, W. Du, Y. Wang, Y. Huang, Q. Yang, Q. Zhang, A novel fluorophore based on the coupling of AIE and ESIPT mechanisms and its application in biothiol imaging, J. Mater. Chem. B 5 (2017) 7736–7742.
[35] Y. Yue, F. Huo, P. Ning, Y. Zhang, J. Chao, X. Meng, C. Yin, Dual-site fluorescent probe for visualizing the metabolism of Cys in living cells, J. Am. Chem. Soc. 139 (2017) 3181–3185.
[36] M. Li, W. Feng, Q. Zhai, G. Feng, Selenocysteine detection and bioimaging in living cells by a colorimetric and near-infrared fluorescent turn-on probe with a large stokes shift, Biosens. Bioelectron. 87 (2017) 894–900.
[37] N. Zhao, Q. Gong, R.X. Zhang, J. Yang, Z.Y. Huang, N. Li, B.Z. Tang, A fluorescent probe with aggregation-induced emission characteristics for distinguishing homocysteine over cysteine and glutathione, J. Mater. Chem. C 3 (2015) 8397–8402.
[38] M.-Z. Zhang, H.-H. Han, S.-Z. Zhang, C.-Y. Wang, Y.-X. Lu, W.-H. Zhu, A new colorimetric and fluorescent probe with a large Stokes shift for rapid and specific detection of biothiols and its application in living cells, J. Mater. Chem. B 5 (2017) 8780–8785.
[39] J. Liu, Y.-Q. Sun, Y. Huo, H. Zhang, L. Wang, P. Zhang, D. Song, Y. Shi, W. Guo, Simultaneous fluorescence sensing of cys and gsh from different emission channels, J. Am. Chem. Soc. 136 (2014) 574–577.
[40] J. Liu, Y.-Q. Sun, H. Zhang, Y. Huo, Y. Shi, W. Guo, Simultaneous fluorescent imaging of Cys/Hcy and GSH from different emission channels, Chem. Sci. 5 (2014) 3183–3188.
[41] H. Zhang, R. Liu, J. Liu, L. Li, P. Wang, S.Q. Yao, Z. Xu, H. Sun, A minimalist fluorescent probe for differentiating Cys, Hcy and GSH in live cells, Chem. Sci. 7 (2016) 256–260.
[42] G.-X. Yin, T.-T. Niu, Y.-B. Gan, T. Yu, P. Yin, H.-M. Chen, Y.-Y. Zhang, H.-T. Li, S.-Z. Yao, A multi-signal fluorescent probe with multiple binding sites for simultaneous sensing of cysteine, homocysteine, and glutathione, Angew. Chem., Int. Ed. 57 (2018) 4991–4994.
[43] S.V. Mulay, Y. Kim, M. Choi, D.Y. Lee, J. Choi, Y. Lee, S. Jon, D.G. Churchill, Enhanced doubly activated dual emission fluorescent probes for selective imaging of glutathione or cysteine in living systems, Anal. Chem. 90 (2018) 2648–2654.
[44] Y.-Q. Sun, J. Liu, J. Zhang, T. Yang, W. Guo, Fluorescent probe for biological gas SO_2 derivatives bisulfite and sulfite, Chem. Commun. 49 (2013) 2637–2639.
[45] X.-L. Liu, L.-Y. Niu, Y.-Z. Chen, Y. Yang, Q.-Z. Yang, A multi-emissive fluorescent probe for the discrimination of glutathione and cysteine, Biosens. Bioelectron. 90 (2017) 403–409.
[46] X. Xia, F. Zeng, P. Zhang, J. Lyu, Y. Huang, S. Wu, An ICT-based ratiometric fluorescent probe for hydrazine detection and its application in living cells and in vivo, Sens. Actuat. B 227 (2016) 411–418.
[47] X. Wang, Z. Guo, S. Zhu, H. Tian, W. Zhu, A naked-eye and ratiometric near-infrared probe for palladium via modulation of a π-conjugated system of cyanines, Chem. Commun. 50 (2014) 13525–13528.
[48] X. Xie, C. Yin, Y. Yue, J. Chao, F. Huo, Fluorescent probe detect distinguishly sulfite/hydrogen sulfide and thiol via two emission channels in vivo, Sens. Actuators, B 277 (2018) 647–653.
[49] L. He, X. Yang, K. Xu, X. Kong, W. Lin, A multi-signal fluorescent probe for simultaneously distinguishing and sequentially sensing cysteine/homocysteine, glutathione, and hydrogen sulfide in living cells, Chem. Sci. 8 (2017) 6257–6265.
[50] Q. Hu, C. Yu, X. Xia, F. Zeng, S. Wu, A fluorescent probe for simultaneous discrimination of GSH and Cys/Hcy in human serum samples via distinctly-separated emissions with independent excitations, Biosens. Bioelectron. 81 (2016) 341–348.
[51] L. Yang, Y. Su, Y. Geng, Y. Zhang, X. Ren, L. He, X. Song, A triple-emission fluorescent probe for discriminatory detection of cysteine/homocysteine glutathione/hydrogen sulfide, and thiophenol in living cells, ACS Sens. 3 (2018) 1863–1869.
[52] W. Chen, H. Luo, X. Liu, J.W. Foley, X. Song, Broadly applicable strategy for the fluorescence based detection and differentiation of glutathione and cysteine/homocysteine: demonstration in vitro and in vivo, Anal. Chem. 88 (2016) 3638–3646.
[53] J. Wang, L. Niu, J. Huang, Z. Yan, X. Zhou, J. Wang, Thiazolyl substituted NBD as fluorescent probe for the detection of homocysteine and cysteine, Dyes Pigm. 158 (2018) 151–156.
[54] Y. Liu, S. Zhang, X. Lv, Y.-Q. Sun, J. Liu, W. Guo, Constructing a fluorescent probe for specific detection of cysteine over homocysteine and glutathione based on a novel cysteine-binding group but-3-yn-2-one, Analyst 139 (2014) 4081–4087.
[55] X. Zhou, X. Jin, G. Sun, X. Wu, A sensitive and selective fluorescent probe for cysteine based on a new response-assisted electrostatic attraction strategy: the role of spatial charge configuration, Chem. - Eur. J. 19 (2013) 7817–7824.
[56] H.S. Jung, J.H. Han, T. Pradhan, S. Kim, S.W. Lee, J.L. Sessler, T.W. Kim, C. Kang, J.S. Kim, A cysteine-selective fluorescent probe for the cellular detection of cysteine, Biomaterials 33 (2012) 945–953.
[57] O. Rusin, N.N. St, Luce, R.A. Agbaria, J.O. Escobedo, S. Jiang, I.M. Warner, F.B. Dawan, K. Lian, R.M. Strongin, Visual detection of cysteine and homocysteine, J. Am. Chem. Soc. 126 (2004) 438–439.
[58] Z. Lu, Y. Lu, C. Fan, X. Sun, M. Zhang, Y. Lu, A two-separated-emission fluorescent probe for simultaneous discrimination of Cys/Hcy and GSH upon excitation of two different wavelengths, J. Mater. Chem. B 6 (2018) 8221–8227.
[59] Z. Lu, W. Fan, Y. Lu, C. Fan, H. Zhao, K. Guo, W. Chu, Y. Lu, A highly sensitive fluorescent probe for bioimaging zinc ion in living cells and zebrafish models, New J. Chem. 42 (2018) 12198–12204.
[60] Y. Yue, F. Huo, F. Cheng, X. Zhu, T. Mafireyi, R.M. Strongin, C. Yin, Functional synthetic probes for selective targeting and multi-analyte detection and imaging, Chem. Soc. Rev. 48 (2019) 4155–4177.
[61] L.-Y. Niu, Y.-S. Guan, Y.-Z. Chen, L.-Z. Wu, C.-H. Tung, Q.-Z. Yang, BODIPY-based ratiometric fluorescent sensor for highly selective detection of glutathione over cysteine and homocysteine, J. Am. Chem. Soc. 134 (2012) 18928–18931.
[62] Y. Qi, Y. Huang, B. Li, F. Zeng, S. Wu, Real-time monitoring of endogenous cysteine levels in vivo by near-infrared turn-on fluorescent probe with large stokes shift, Anal. Chem. 90 (2018) 1014–1020.
[63] S. Gao, Y. Tang, W. Lin, Development of a two-photon turn-on fluorescent probe for cysteine and its bio-imaging applications in living cells, tissues, and zebrafish, New J. Chem. 42 (2018) 14075–14078.
[64] Z. Lu, W. Fan, X. Shi, Y. Lu, C. Fan, Two distinctly separated emission colorimetric NIR fluorescent probe for fast hydrazine detection in living cells and mice upon independent excitations, Anal. Chem. 89 (2017) 9918–9925.
[65] L. He, X. Yang, K. Xu, Y. Yang, W. Lin, A multifunctional logic gate by means of a triple-chromophore fluorescent biothiol probe with diverse fluorescence signal patterns, Chem. Commun. 53 (2017) 13168–13171.